Brazilian Journal
of Chemical
Engineering

ISSN 0104-6632
Printed in Brazil
www.abeq.org.br/bjche

Vol. 33, No. 04, pp. 1055 - 1061, October - December, 2016
dx.doi.org/10.1590/0104-6632.20160334s20150023

EFFECT OF OIL TEMPERATURE ON THE WAX DEPOSITION OF CRUDE OIL WITH COMPOSITION ANALYSIS

Qing Quan[1], Wei Wang[1], Pengyu Wang[2], Juheng Yang[1], Ge Gao[1], Lu Yang[1] and Jing Gong[1*]

[1]Beijing Key Laboratory of Urban Oil & Gas Distribution Technology,
China University of Petroleum, 102249, Beijing, China.
Phone: + 86-10-8973-2156
[*]E-mail: ydgj@cup.edu.cn
E-mail: qingqing.lf@163.com; w.wang@cup.edu.cn; yangjuheng@126.cm;
gaoge_cup@163.com; yanglu.shan@163.com
[2]Petro China Pipeline R&D Center, 065000, Hebei, China.
E-mail: pengyuwang@hotmail.com

(Submitted: January 16, 2015 ; Revised: March 20, 2015 ; Accepted: July 16, 2015)

Abstract - Wax deposition behavior was investigated in a set of one-inch experiment flow loops, using a local crude oil with high wax content. The temperature of the oil phase is chosen as a variable parameter while the temperature of the coolant media is maintained constant. Detailed composition of the deposit is characterized using High Temperature Gas Chromatography. It was found that the magnitude of the diffusion of the heavier waxy components (C_{35}-C_{50}) decreases when the oil temperature decreases, but the magnitude of the diffusion of the lighter waxy components increases. This result means that the diffusion of wax molecules shifts towards lower carbon number, which further proves the concept of molecular diffusion. Meanwhile, a meaningful phenomenon is that the mass of the deposit increases with the oil temperature decrease, which definitely proves the influence of wax solubility on deposition, while the formation of an incipient gel layer reflects the fact that an increase in the mass of the deposit does not mean a larger wax percentage fraction at lower oil temperature.
Keywords: Wax deposition; Molecular diffusion; Incipient gel layer; Crude oil.

INTRODUCTION

Wax deposition is a crucial problem to be solved in crude oil flow assurance for inland and offshore pipelines. The accumulation of the deposit may lead to increased pumping power, decreased flow rate or even to the total blockage of the pipeline. Factors that contribute to wax deposition in pipelines include: temperature, flow rate, oil composition, thermal history, time, etc (Bern *et al*., 1980; Burger *et al*., 1981; Majeed *et al*., 1990; Hamouda and Ravnoy, 1992; Weingarten and Euchner, 1988; Lu *et al*., 2011). Various mechanisms have been proposed during the past decades, including molecular diffusion, shear dispersion, gravity settling, Brownian diffusion, etc. Molecular diffusion and aging effects have been supported as the predominant mechanisms, which clearly explain the flow rate effect and enrichment of heavy components in the deposit with time (Singh *et al*., 2000; Singh *et al*., 2001; Hernandez *et al*., 2004).

Experimental studies on wax deposition have shown that the difference between the crude oil and ambient temperatures is a more important parameter for wax deposition. Huang *et al*. (2011) suggested that the shape of the solubility curve, which affects the change in characteristic mass flux, is the major

*To whom correspondence should be addressed

factor to explain the effect of oil temperature on the deposit. Lashkarbolooki *et al*. (2011) found that the deposit thickness is a function of temperature difference, where the deposit thickness obviously decreases but the wax percentage fraction increases at small temperature difference. An increase in the mass of the deposit does not accordingly mean a larger wax percentage fraction. Valinejad and Nazar (2013) revealed that the temperature difference between the oil and pipe wall has the maximum percentage of contribution to the amount of deposited wax. Waxy crude oil with higher wax content could lead to more deposited solid wax.

Meanwhile, the deposit composition varies with time and becomes harder upon aging. Singh *et al*. (2000; 2001) proposed that wax molecules having a carbon number larger than a critical value diffuse into the gel deposit, while a reverse diffusion of lighter molecules out of the deposit results in the increase of the wax content in the gel deposit. Merino-Garcia *et al*. (2007) proved that the gelling effect leads to a quick formation of a loose solid network, and this incipient gel deposit is later concentrated by molecular diffusion in a successive step. Parthasarathi and Mehrotra (2005) found that the majority of the deposit occurred in a short initial period, and there was only a slight increase in the deposit with longer time.

The effect of oil to wall temperature difference is important to better understand the wax deposition phenomenon. However, wax deposition is a complex problem due to high variation in the properties of crude oil. Further studies are required to provide information on why an increase in the total amount of deposit does not accordingly mean a larger wax percentage fraction (Lashkarbolooki *et al*., 2011). In the present work, the pipe wall temperature is kept constant, while the oil temperature is chosen as a variable parameter. The influence of oil temperature on the amount of deposited wax and its composition are evaluated. It was found that the magnitude of the diffusion of the heavier waxy components (C_{35}-C_{50}) decreases, but the diffusion of the lighter waxy components increases with the oil temperature decrease.

EXPERIMENTAL METHODS

Experiment Apparatus

The wax deposition flow loop consists of the oil supply, measuring, temperature control, test section, reference section, and data acquisition systems, as shown Figure 1. The flow loop is a horizontal circuit 25 meters long, 1 inch inner diameter, using DN25 stainless steel tube. The lengths of the test and reference sections are both 2 meters, equipped with differential pressure transducers with a measurement accuracy of 0.075%. The volume of the supply oil tank is 0.34 m^3 to minimize the influence of wax loss during deposition. The temperature of the oil tank and flow loop is monitored online by water circulation in the outer jacket of the oil tank and pipe sections. Temperature sensors are placed at the pump discharge, inlet and outlet of the test section, reference section and each water jacket. The oil-feed pump is a helical rotor pump with maximum flow rate of 3.3 m^3/h and pressure 2.4 MPa.

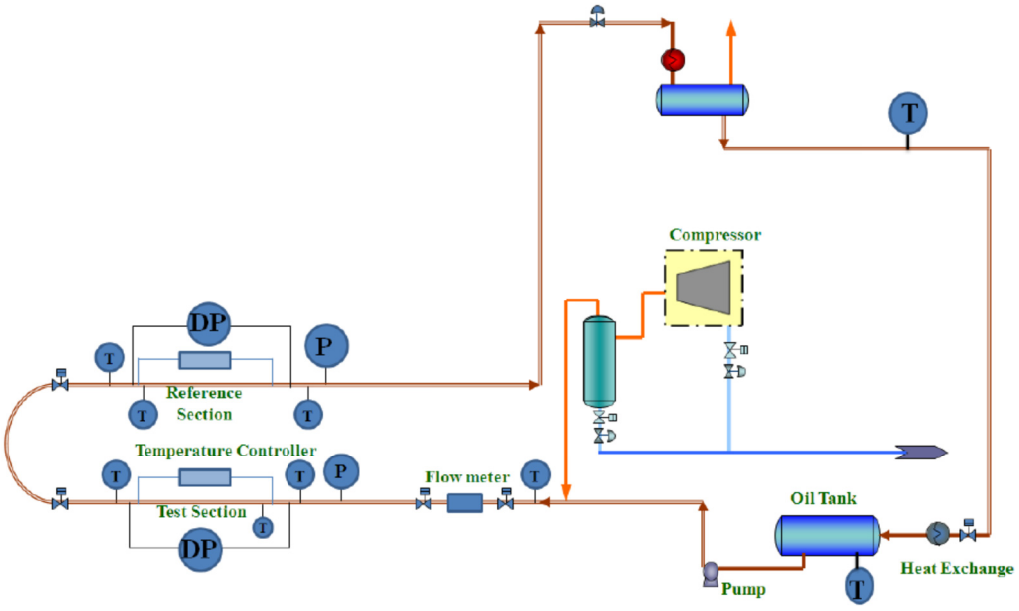

Figure 1: The schematic map of the flow loop.

Materials and Procedures

The oil phase used in the experiments is a crude oil from China with high wax content (density 864.4 kg/m^3 at 40 °C, wax content 27.5%, WAT 45.8 °C, gel point 38 °C). The wax content and WAT are measured with a Differential Scanning Calorimeter (DSC, TA2000/MDSC2910) with 0.1 μW of heat flux accuracy and 0.1 °C of the temperature-controlled accuracy. During a DSC analysis, the crude sample is first heated to 80 °C, held at this temperature for 1 min and then cooled from 80 to -30 °C at a rate of 5 °C/min. In this process, a thermal profile was recorded by computer to show the relationship between heat influx and the programmed temperature. In the thermal profile, the temperature point at which the heat flux started to deviate from the baseline was the so-called WAT. At this temperature, the dissolved waxes started to crystallize, simultaneously releasing latent heat. The integral area between the heat flow curve and the horizontal baseline from WAT to -20 °C was integrated to calculate the total latent heat of wax crystallization. With the average crystal enthalpy of wax, the wax content of the sample was obtained. In this study, the final wax content of the deposit adopted the average value of the results from three repeated experiments for each operating condition with good reproducibility (Wang and Huang, 2014). Figure 2 provides the measured viscosity at different shear rates and temperatures (Anton Paar MCR301).

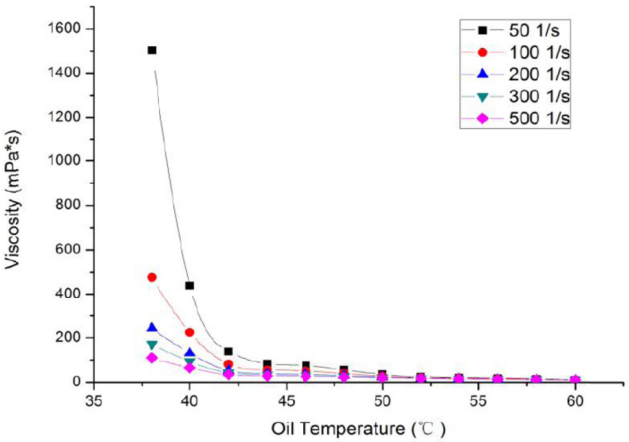

Figure 2: Viscosity vs. temperature and shear rate.

To guarantee the reproducibility of experiments, the crude oil is pretreated for 6 hours at 70 °C to ensure that wax crystals had sufficiently dissolved. Temperatures of the flow loop are controlled at the experimental temperatures. The coolant temperature at the test section was kept at 38 °C, while the temperature of entrance oil in the test section was varied from 50 to 41 °C. The flow rate analyzed was 2000 kg/h (laminar flow) and the deposition period 24 h.

Wax Thickness Measurement

Pressure Difference Method

The hydraulic diameter in the test section will be reduced by the process of wax deposition, resulting in the increase of the pressure drop gradient. Online monitoring of the change in pressure difference can help to calculate the deposit thickness (Parthasarathi and Mehrotra, 2005; Anosike, 2007). The pressure difference of the pipe section can be expressed as:

$$\Delta P = \lambda \frac{L}{D}\frac{\rho V^2}{2} = \frac{8\lambda L \rho Q^2}{\pi^2 D^5} \tag{1}$$

where ΔP is the differential pressure for a horizontal pipeline (Pa); λ is the hydraulic friction coefficient; L is the length of the horizontal pipeline (m); D is the inner diameter of the horizontal pipeline (m); ρ is the density of the fluid (kg/m^3); V is the velocity of the fluid (m/s); Q is the volume flow rate of the fluid (m^3/s). According to Eq. (1), the ratio of the pressure drop between test section and reference section can be expressed as:

$$\frac{\Delta P_T}{\Delta P_R} = \left(\frac{\lambda_T}{\lambda_R}\right)\left(\frac{L_T}{L_R}\right)\left(\frac{\rho_T}{\rho_R}\right)\left(\frac{Q_T}{Q_R}\right)^2\left(\frac{D_R}{D_T}\right)^5 \tag{2}$$

The subscripts T and R represent the parameters of the test section and reference section, respectively. The temperatures of the oil flow in the two sections are nearly the same, so $\rho_T = \rho_R$, $L_T = L_R$, $Q_T = Q_R$, and Eq. (2) can be simplified as:

$$\frac{\Delta P_T}{\Delta P_R} = \left(\frac{\lambda_T}{\lambda_R}\right)\left(\frac{D_R}{D_T}\right)^5 \tag{3}$$

In laminar flow: 1) For a Newtonian fluid, $\lambda = \frac{64}{\mathrm{Re}}$, $\mathrm{Re} = \frac{\rho D V}{\mu}$, where μ is the dynamic viscosity (Pa.s). The average deposit thickness for Newtonian fluid can be calculated by Eq. (4),

$$D_T = D_R \Big/ \left(\frac{\Delta P_T}{\Delta P_R}\right)^{0.25} \tag{4}$$

2) For a non-Newtonian fluid, $\lambda=\frac{64}{\mathrm{Re}_{MR}}$, $\mathrm{Re}_{MR}=\rho D^n V^{2-n}\Big/\frac{K}{8}\left(\frac{6n+2}{n}\right)^n$, where K is the consistency coefficient; n is the index of flow characteristics. The average deposit thickness for a non-Newtonian fluid can be calculated by Eq. (5),

$$D_T = D_R \Big/ \left(\frac{\Delta P_T}{\Delta P_R}\right)^{\left(\frac{1}{3n+1}\right)} \tag{5}$$

Volume Method

After each set of experiments, the test section is disassembled from the flow loop and placed vertically with one end sealed. Water is replaced in the test section to determine the average thickness of the deposit. Samples of the deposit are scraped from the test section for further composition analysis.

Composition Analysis

A high-temperature gas chromatograph (HTGC, Agilent 7890A) with a capillary column HT750 was used for composition analysis. Samples are dissolved in carbon disulfide and the solutions are injected onto the column using an auto-sampler. The carrier gas used was nitrogen with a flow rate of 1 mL/min. The oven temperature is initiated at 50 °C and increases to 430 °C at a rate of 10 °C/min. The solutions are measured three times and an average composition is determined.

RESULTS AND DISCUSSION

During the experiment, the temperature of the coolant in the test section remained 38 °C, and the oil temperature varied from 50 °C to 41 °C. The flow regime was maintained in laminar flow, and the time for each set of deposition kept at 24 h. The influence of oil temperature on the total amount of deposit and its compositions variation were investigated with the coolant temperature of the test section set at the gel point of the crude oil (38 °C), and the contribution of the incipient gel layer and molecular diffusion on the amount of deposition is further discussed.

Comparing the deposit composition measured by HTGC, it was found that the percentage weight of heavier components in the deposit (C_{35}-C_{50}) decreased with the decrease of oil temperature from 50 °C to 41 °C, and gradually became similar to that of the crude oil, as shown in Figure 3. The deposit formed at 50 °C shows obvious peaks, with the weight ratio of C_{35}-C_{50} in the deposition being the highest. This is reasonable since the decrease in oil temperature will inhibit the precipitation of higher molecular weight wax molecules and these precipitated waxes will not be deposited driven by molecular diffusion.

Interestingly, the components of C_{28}-C_{35} in the deposit formed at 44 °C oil temperature are higher than at other temperatures. A similar trend of peak C_{20}-C_{27} percentage weight in the deposit occurs at 41 °C oil temperature. It can be clearly observed from Fig. 3 that the magnitude of the diffusion of lighter waxy components increases as the oil temperature decreases. These findings indicate that the diffusion of wax molecules shifts towards lower carbon number at lower oil temperature, which indeed supports the concept of wax deposition driven by molecular diffusion.

As seen in Figure 4, the deposit thickness increases with the decrease in oil temperature; the radial temperature gradient (dT/dr) decreases and the oil viscosity increases to hinder molecular diffusion.

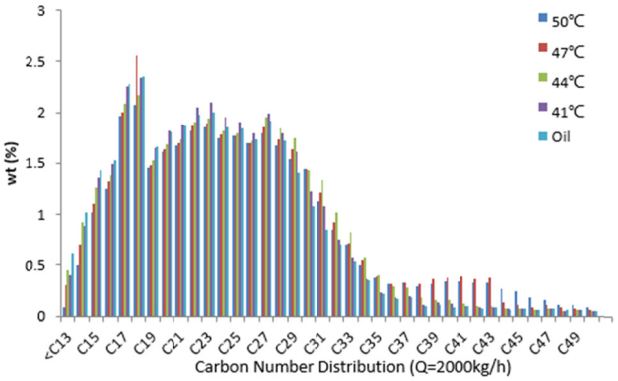

Figure 3: HTGC results of deposit layer at oil temperature 50 °C to 41 °C.

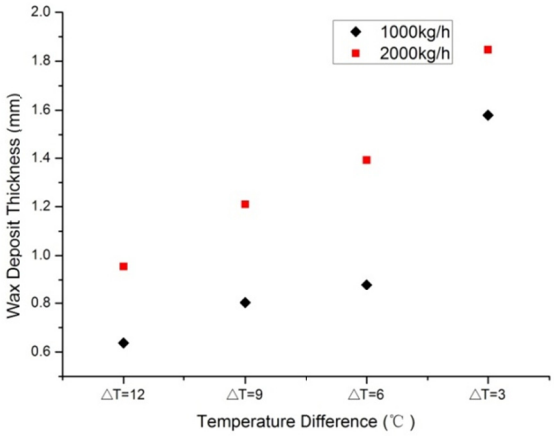

Figure 4: Comparisons between the measured and predicted deposit thickness.

Based on the two-dimensional heat transfer model as shown in Eqs. (6)-(7) (Huang *et al*., 2011), the radial temperature of the test section inlet was calculated and compared in Figure 5.

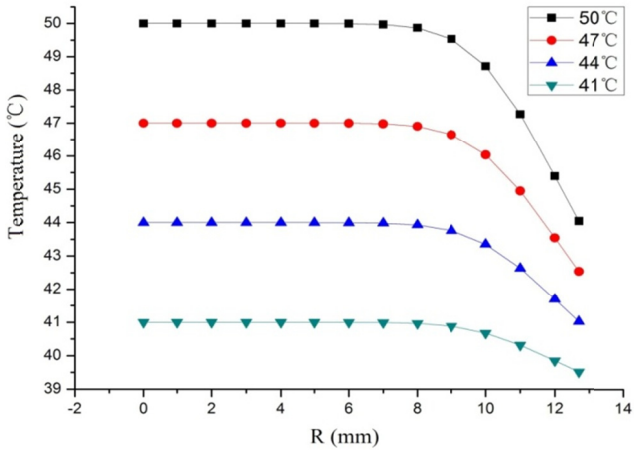

Figure 5: Calculated radial temperature profile at 2000 kg/h flow rate (X axial: 0 mm-pipe center, 12.7 mm-pipe inner wall).

Heat transfer:

$$V_Z \frac{\partial T}{\partial z} = \frac{1}{r}\frac{\partial}{\partial r}\left[r(\varepsilon_H + \alpha_T)\frac{\partial T}{\partial r} \right] \tag{6}$$

Boundary conditions:

$$\begin{cases} T = T_b, \text{ at } z=0 \\ \dfrac{\partial T}{\partial r} = 0, \text{at } r=0 \\ h_0(T_{coolant} - T_{wall}) = \lambda_{dep}\dfrac{\partial T}{\partial r}, \text{at } r=R \end{cases} \tag{7}$$

where V_z is the average velocity of oil on the axial coordinate (m/s); T is the temperature (°C); r is the radial coordinate (m); z is the axial coordinate (m); R is the radius of pipeline (m); T_b is inlet temperature (°C); ε_H is the eddy diffusivity for energy (m^2/s), ε_H=0 in laminar flow; α_T is the thermal difusivity of crude oil (m^2/s); h_0 is the external heat transfer coefficient (W/m^2/°C); λ_{dep} is the effective thermal conductivity of the gel (W/m/°C).

The results of deposit thickness in Fig. 4 seem to be inconsistent with the decreased radial temperature gradient in Fig. 5. However, it actually supports a current finding by Huang *et al*. (2011) that the solubility curve of the oil phase will have an obvious influence on the forming of wax deposition. Checking the detailed composition of the crude oil in Fig. 3, it is quite different from a mono-component hydrocarbon wax. Its composition covers a wide range of carbon numbers from C_{14} to C_{50}, where carbon numbers C_{15} to C_{30} make up a high percentage of the weight with over 1% individually and higher molecular weight hydrocarbons (>C_{30}) co-exist. Therefore, despite the radial temperature gradient decrease, it is reasonable that a decrease in the oil temperature would result in the precipitation of lower molecular weight hydrocarbons, the formation of a lower molecular concentration gradient and less deposit. This is in accordance with the HTGC results of deposit composition shift towards lower carbon number at lower oil temperature. Combined with the mass transfer equation shown in Eqs. (8)-(9) (Huang *et al*., 2011), the predicted mass diffusion coefficient of wax in oil (D_{wo}), the oil to wall concentration difference of wax molecules (C_{oil}-C_{wall}) and the characteristic mass flux for wax deposition (J_{wax} = D_{wo} *(C_{oil}-C_{wall})) at various oil temperatures are compared in Table 1 and Figure 6.

Mass transfer: $$V_Z \frac{\partial C}{\partial z} = \frac{1}{r}\frac{\partial}{\partial r}\left[r\left(\varepsilon_m + D_{wo}\right)\frac{\partial C}{\partial r} \right] \tag{8}$$

Boundaries: $$\begin{cases} C = C_b, \text{ at } z=0 \\ \dfrac{\partial C}{\partial r} = 0, \text{at } r=0 \\ C = C_{ws}(T), \text{at } 0 < r \le R \end{cases} \tag{9}$$

where C is the concentration of wax in the oil (wt%); ε_m is the eddy diffusivity for mass (m^2/s), ε_m=0 in laminar flow; D_{wo} is the mass diffusion coefficient of wax in oil (m^2/s).

Table 1: Parameters for the mass diffusion coefficient of wax in oil, D_{wo}, equilibrium concentration of wax, C, and the characteristics of mass flux for wax deposition, J_{wax}.

Parameters	Values			
	Experimental Operating Conditions			
T_{oil}, °C	50	47	44	41
$T_{coolant}$, °C	38	38	38	38
ΔT, °C	12	9	6	3
Q_{oil}, kg/h	2000	2000	2000	2000
WAT, °C	45.8	45.8	45.8	45.8
	Model Predictions			
T_{wall}, °C	44	42.5	41	39.5
$D_{wo,wall}$ *10^{10}, m^2/s	0.564	0.51	0.347	0.227
C_{oil}, wt%	27.5	27.5	27.42	26.18
C_{wall}, wt%	27.42	27	26.18	25
C_{oil},- C_{wall}, wt%	0.08	0.5	1.24	1.18
J_{wax}*10^{10}, m/s·wt%	0.045	0.255	0.43	0.268

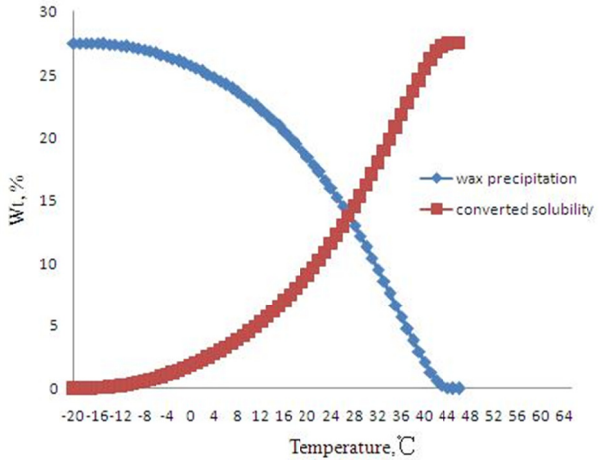

Figure 6: Amount of precipitated wax in oil at various temperatures and the corresponding solubility curve for the crude oil.

It is obvious that the predicted characteristics of mass fluxes (J_{wax}) at 50, 47, and 44 °C are in good accordance with the experimentally measured deposit thickness, which definitely proves the influence of wax solubility on deposit in the complex crude oil system, though the mass diffusion coefficient D_{wo} decreases with the diminished temperature difference dT/dr. However, the predicted J_{wax} experiences a decrease at 41 °C, which is inconsistent with the measured one. A possible explanation is the formation of an incipient gel layer at relatively lower oil temperature during laminar flow (Anosike, 2007).

The measured online pressure gradients are compared at 41 °C and 50 °C oil temperatures during the forming of wax deposition, as shown in Figure 7. The pressure drop gradient experiences an initial increase trend, and then gradually become smooth after 15h. Among all the temperatures studied, the pressure drop gradient exhibited the sharpest trend at 41 °C, which indicates the quickest deposition rate in the initial period. As presented in Table 1, the diffusion coefficient of wax molecules D_{wo} and the diffusion mass flux J_{wax} both decrease; the possible reasons are provided as follows:

1) When the oil temperature is 41 °C, the wall temperature is around 39.5 °C. The prediction result in Table 1 confirms that almost 2.5 wt% waxes precipitate near the wall surface. Compared to the 0.5 wt% and 1.32 wt% wax crystals at 47 and 44 °C oil temperatures, it is reasonable that the wax crystals form the 3D network structure at 41 °C oil temperature and build up the incipient gel layer near the pipe wall in which oil phase is trapped.

2) When the oil temperature is 41 °C, the viscosity of the oil phase near the pipe wall is around 600 mPa.s at 50 s^{-1} shear rate, which is nearly two times that at 44 °C oil temperature. It would further help to enhance the gelling probability near the pipe wall.

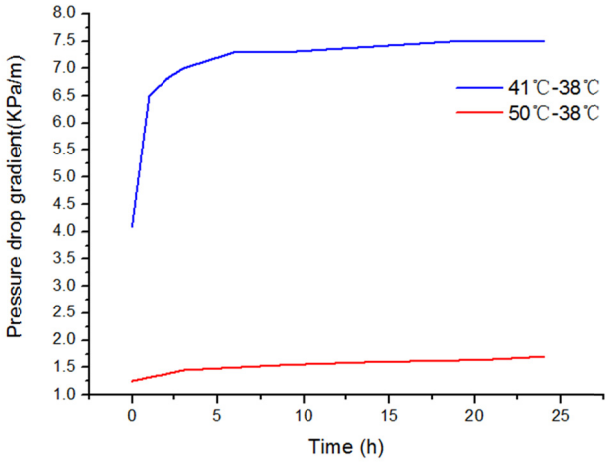

Figure 7: The vibration of the differential pressure signal with time under different temperature conditions.

Thus, the forming of an incipient gel layer results in a quick increasing trend of measured pressure gradient in Fig. 6, which further reflects the essence of why an increase in the total amount of deposit (Fig. 4) does not accordingly mean a larger wax percentage fraction (Table 1).

CONCLUSION

Wax deposition behavior has been investigated using a local Chinese crude oil with high wax content. The temperature of the cooling liquid remains constant, while the oil temperature is chosen as a variable parameter. The influence of oil temperature on the amount of deposited wax and its composition are discussed. It is found that the magnitude of diffusion of the heavier components decreases when the oil temperature decreases, and the diffusion of wax molecules shifts towards lower carbon number. The mass of deposit increases with the oil temperature decrease, which proves the influence of the solubility curve on deposition, especially in the complex crude oil system.

ACKNOWLEDGEMENT

The authors wish to thank the National Science & Technology Specific Project (2011ZX05026-004), the Program for New Century Excellent Talents in University (NCET-12-0969), the Foundation for the Author of National Excellent Doctoral Dissertation

of PR China (201254), and the National Natural Science Foundation of China (51422406) for providing support for this work.

REFERENCES

Anosike, C. F., Effect of flow patterns on oil−water flow paraffin deposition in horizontal pipes. Tulsa (2007).

Bern, P. A., Withers, V. R. and Cairns, J. R., Wax deposition in crude oil pipelines. Proceedings of the European Offshore Petroleum Conference. London (1980).

Burger, E. D., Perkins, T. K. and Striegler, J. H., Studies of wax deposition in the trans Alaska pipeline. Journal Petroleum Technology, 33, 1075-1086 (1981).

Merino-Garcia, D., Michele, M. and Sebastiano, C., Kinetics of waxy gel formation from batch experiments. Energy Fuels, 21, 1287-1295 (2007).

Hamouda, A. A. and Ravnoy, J. M., Prediction of wax deposition in pipelines and field experience on the influence of wax on drag-reducer performance. 24th Annual Offshore Technical Conference. Houston (1992).

Huang, Z., Lu, Y., Hoffmann, R., Amundsen, L. and Fogler, H. S., The effect of operating temperatures on wax deposition. Energy Fuels, 25, 5180-5188 (2011).

Hernandez, O. C., Hensly, H., Sarica, C., Brill, J. P., Volk, M. and Delle, E., Improvements in single phase paraffin deposition modeling. SPE, 11, 237-244 (2004).

Lu, Y., Huang, Z., Hoffmann, R., Amundsen, L. and Fogler, H. S., Counterintuitive effects of the oil flow rate on wax deposition. Energy Fuels, 26, 4091-4097 (2011).

Lashkarbolooki, M., Seyfaee, A., Esmaeilzadeh, F., Mowla, D., Experimental investigation of wax deposition in Kermanshah crude oil through a monitored flow loop apparatus. Energy Fuels, 24, 1234-1241 (2011).

Majeed, A., Bringedal, B. and Overa, S., Model calculates wax deposition for N. Sea oils. Oil & Gas Journal, 88, 63-69(1990).

Parthasarathi, P. and Mehrotra, A. K., Solids deposition from multi-component wax solvent mixtures in a bench scale flow-loop apparatus with heat transfer. Energy Fuels, 19, 1387-1398 (2005).

Singh, P., Venkatesan, R., Fogler, H. S. and Nagarajan, N. R., Formation and aging of incipient thin film wax/oil gels. AIChE J., 46, 1059-1073 (2000).

Singh, P., Venkatesan, R., Fogler, H. S. and Nagarajan, N. R., Morphological evolution of thick wax deposits during aging. AIChE J., 47(1), 6-18 (2001).

Valinejad, R. and Nazar, A. R., An experimental design approach for investigating the effects of operation factors on the wax deposition in pipelines. Fuel, 106, 843-850 (2013).

Weingarten, J. S. and Euchner, J. A., Methods for predicting wax precipitation and deposition. SPE, 3, 121-126 (1988).

Wang, W. and Huang, Q., Prediction for wax deposition in oil pipelines validated by field pigging. Journal of the Energy Institute, 87, 196-207 (2014).